Supporting Information

Photocytotoxic luminescent lanthanide complexes of DTPA– bisamide using quinoline as photosensitizer

Khushbu Singh,[†] *Samya Banerjee*[‡] *and Ashis K. Patra*[*,†]

[†]Department of Chemistry, Indian Institute of Technology Kanpur, Kanpur 208016, Uttar Pradesh, India

[‡]Department of Inorganic and Physical Chemistry, Indian Institute of Science, Bangalore 560012, Karnataka, India

*E-mail: akpatra@iitk.ac.in

Table of Contents

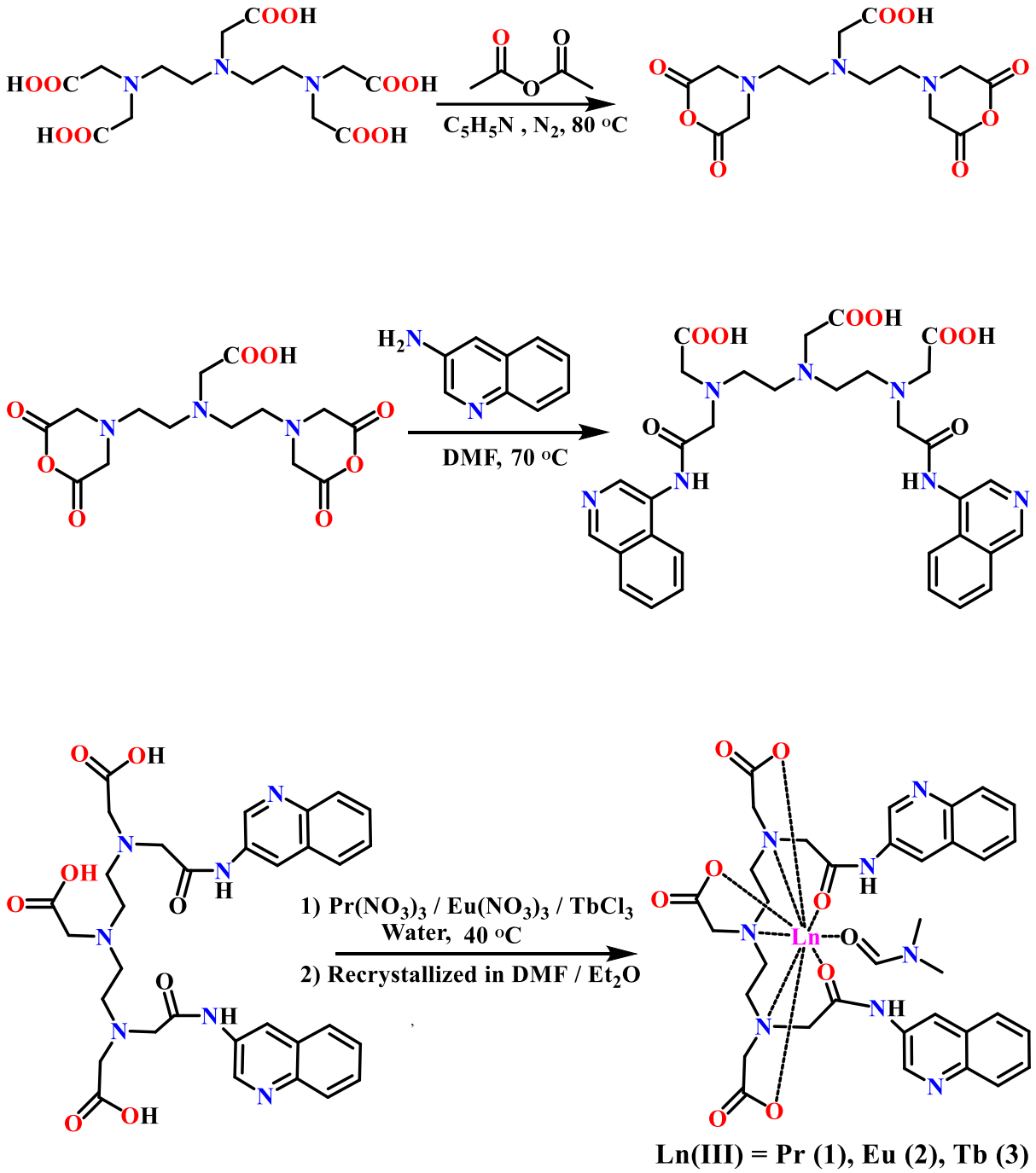

Scheme S1. General synthetic scheme for H_3DTPAAQ ligand and complexes **1-3**.

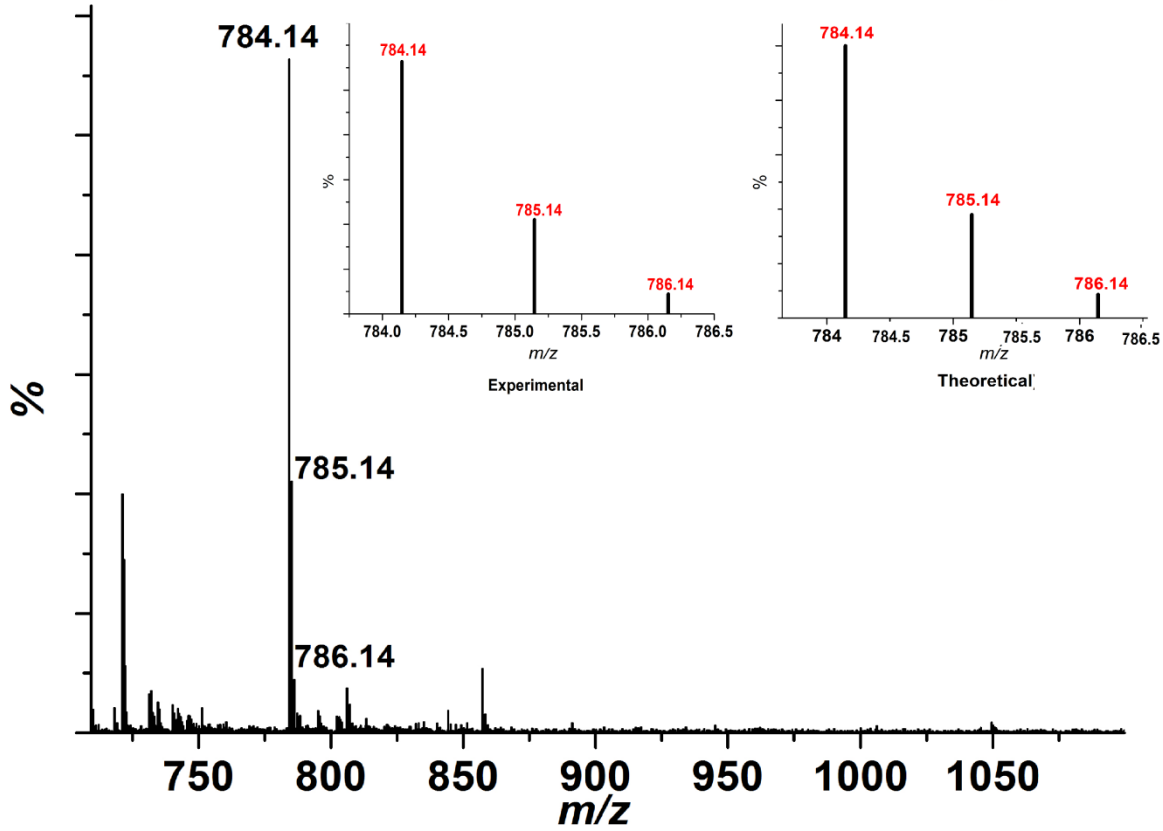

Figure S1. ESI-MS of complex **1** in aqueous-DMF: *m/z* [(**1**–DMF + H]$^+$ calcd. for $C_{32}H_{32}N_7O_8Pr$ (relative abundance): 784.14 (100.0%), 785.14 (37.93%), 786.14 (8.5%). Found: 784.14 (100.0%), 785.14 (39.82%), 786.14 (7.8%).

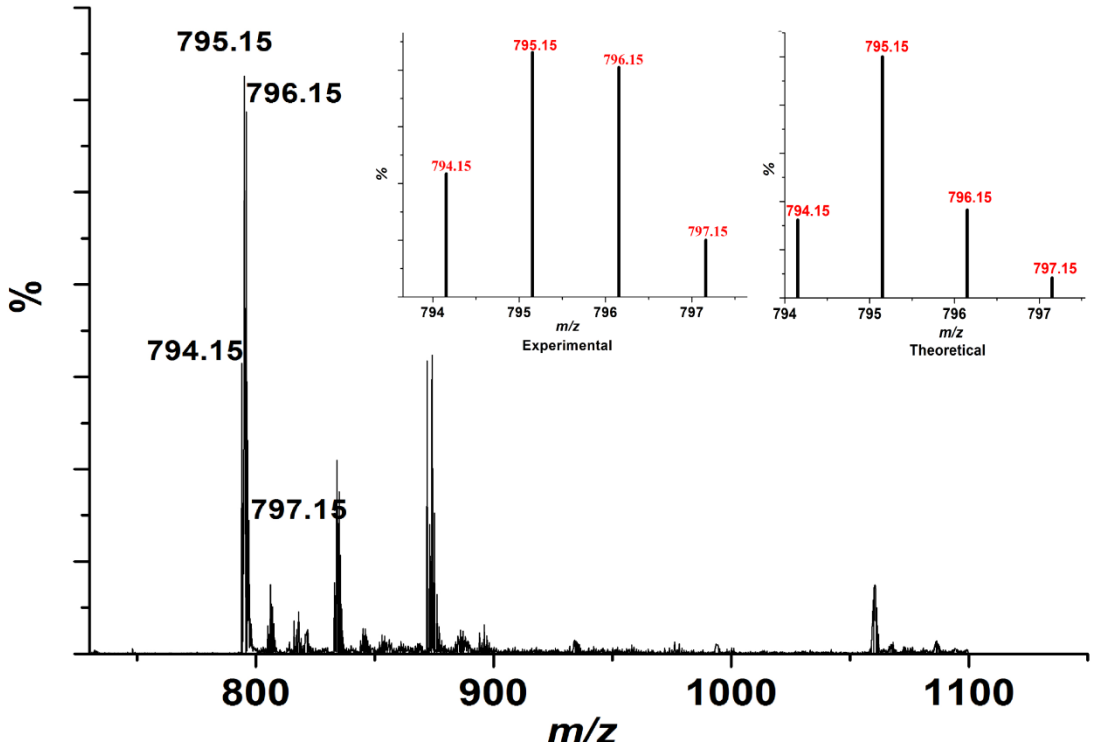

Figure S2. ESI-MS of complex **2** in aqueous DMF: *m/z* [**2** – DMF + H]$^+$; calcd. for $C_{32}H_{32}N_7O_8Eu$ (relative abundance): 795.15 (100.0%), 794.15 (38.2%), 796.15 (45.5%), 797.15 (3.3%). Found: 795.15 (100.0%), 794.15 (90.8%), 796.15 (36.1%), 797.15 (7.8%).

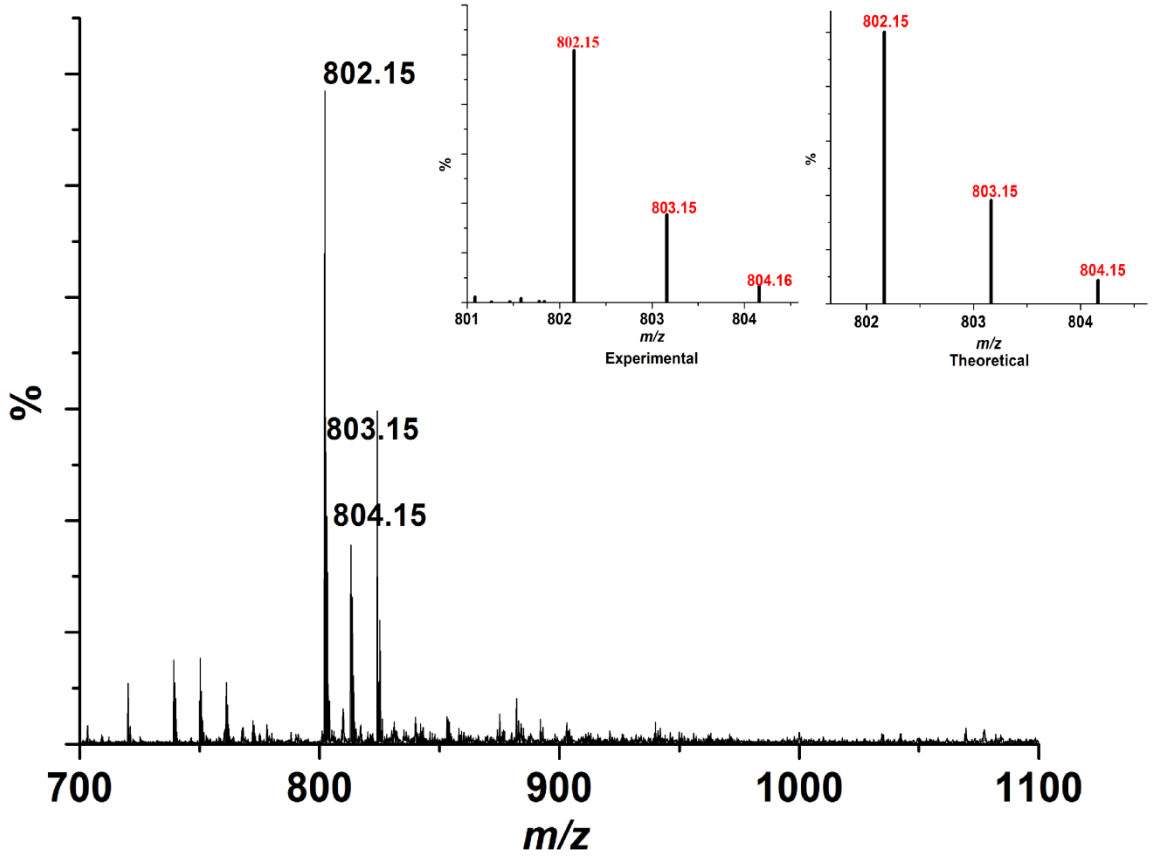

Figure S3. ESI-MS of complex **3** in aqueous DMF: *m/z* [**3**–DMF + H]$^+$; calcd. for $C_{33}H_{35}N_7O_8Tb$ (relative abundance): 802.15 (100.0%), 803.15 (35.3%), 804.15 (8.5%). Found: 802.15 (100.0%), 803.15 (37.5%), 804.15 (7.5%).

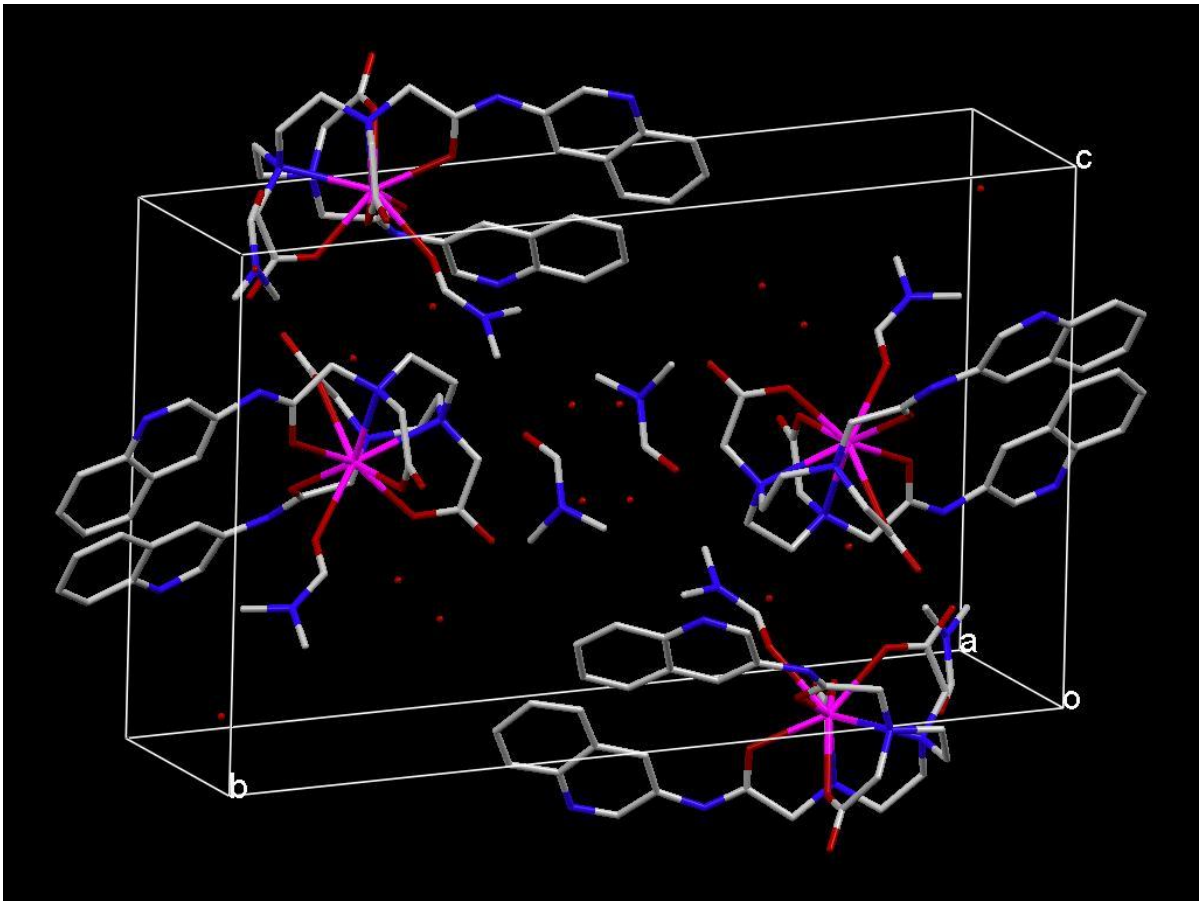

Figure S4. Unit cell packing diagram of [Pr(DTPAAQ)(DMF)] (**1**) along b-axis.

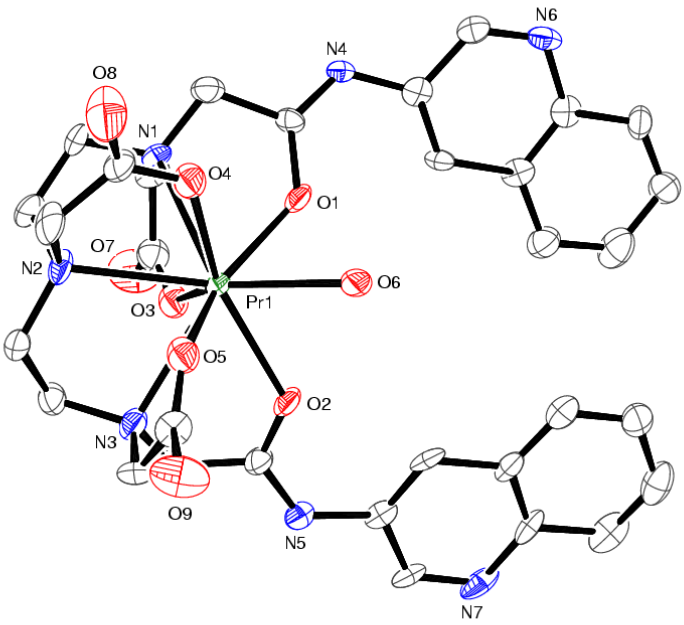

Figure S5. ORTEP view of [Pr(DTPAAQ)(H_2O)] (**1a**) with 50% probability thermal ellipsoid with atom labelling scheme for the metal and heteroatoms.

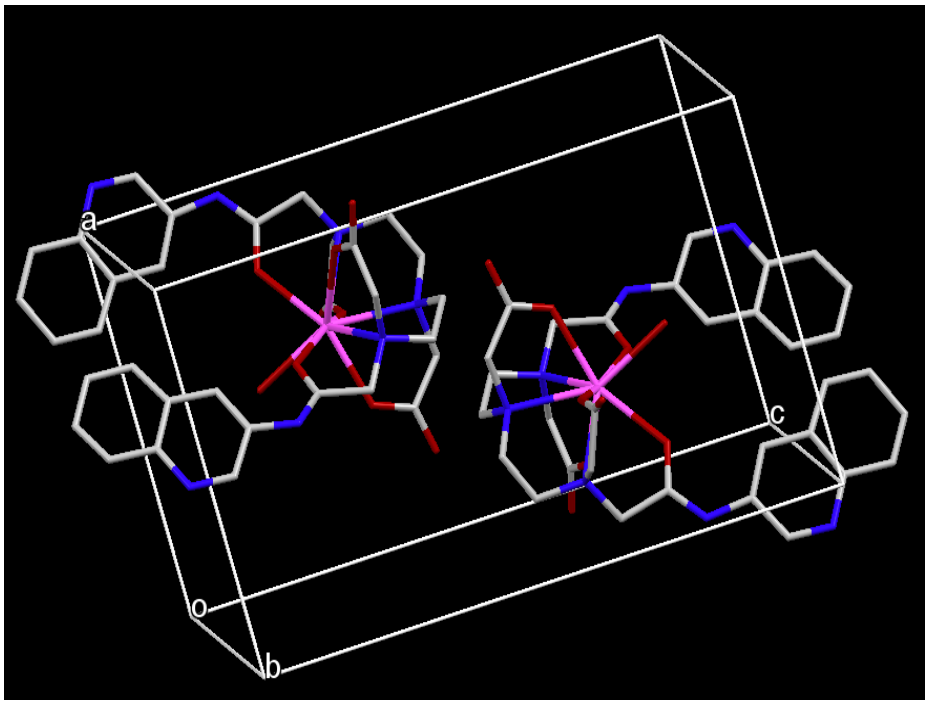

Figure S6. Unit cell packing diagram of [Pr(DTPAAQ)(H_2O)] (**1a**) along b-axis.

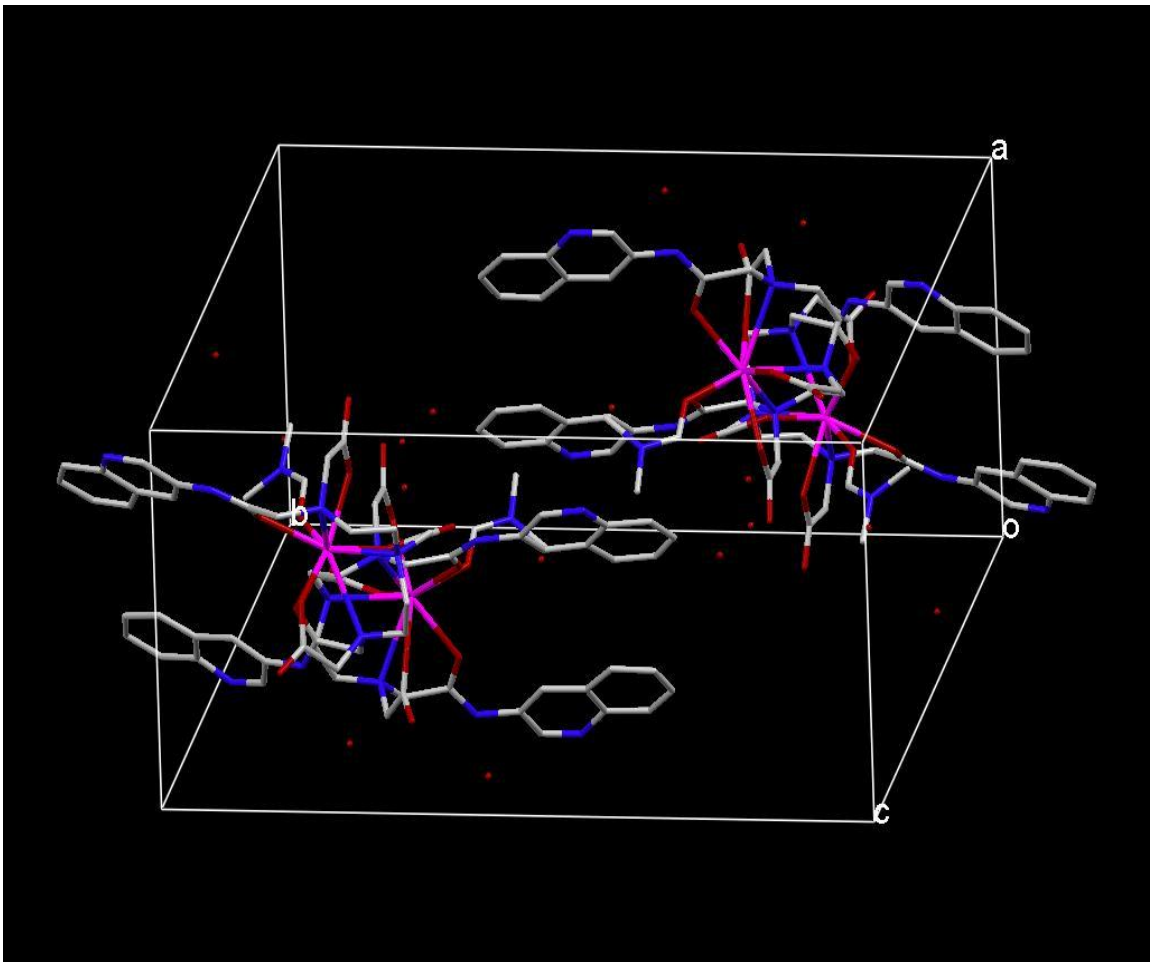

Figure S7. Unit cell packing diagram of [Eu(DTPAAQ)(DMF)] (**2**) along b-axis.

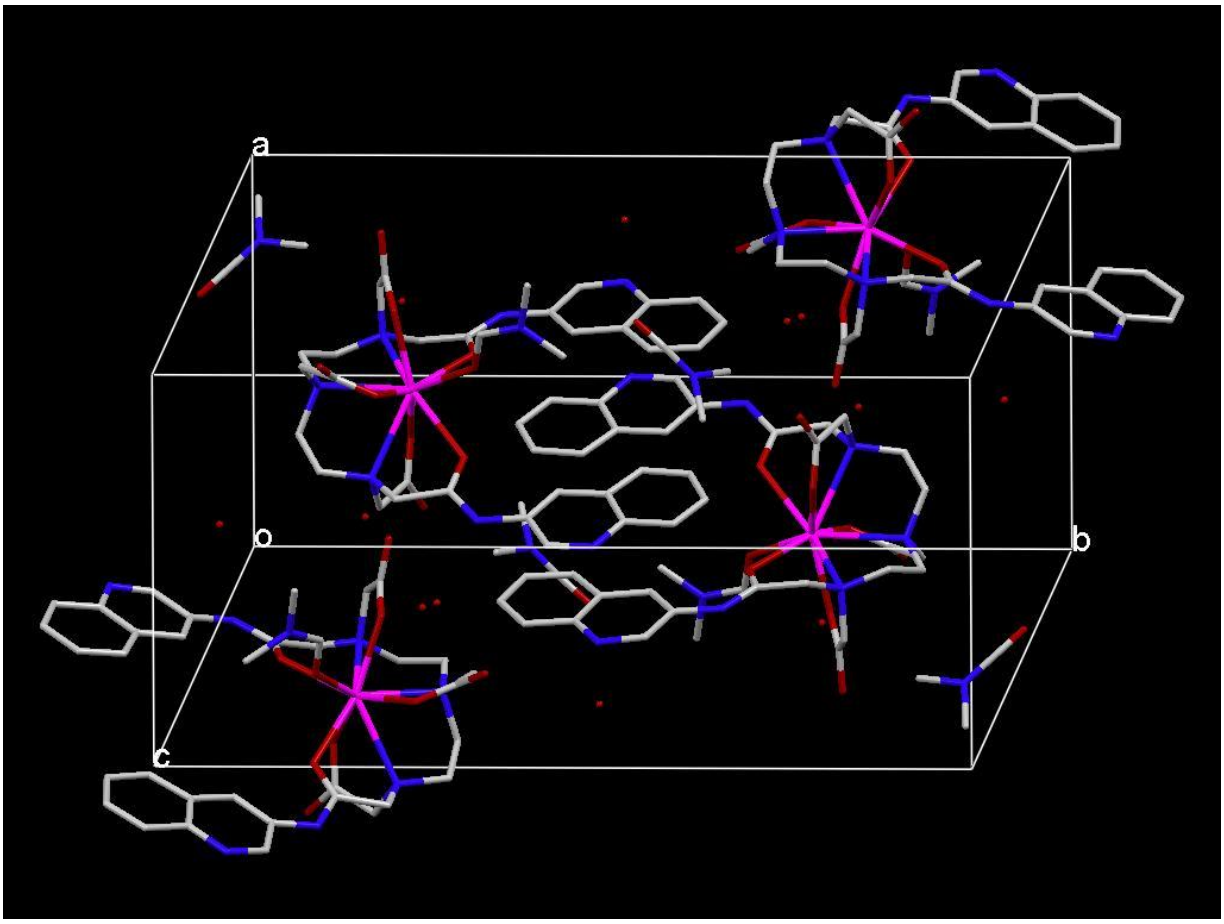

Figure S8. Unit cell packing diagram of [Tb(DTPAAQ)(DMF)] (**3**) along b-axis.

Table S1.Crystal data and structural refinement details for complexes **1a** and **1-3**.

Parameters	**1·DMF·4H$_2$O**	**1a**	**2·4H$_2$O**	**3·DMF·3H$_2$O**
Empirical Formula	$C_{38}H_{54}N_9O_{13}Pr$	$C_{32}H_{34}N_7O_9Pr$	$C_{35}H_{41}N_8O_{13}Eu$	$C_{38}H_{52}N_9O_{13}Tb$
Formula weight	985.81	801.57	933.72	1001
Crystal system	Monoclinic	Triclinic	Monoclinic	Monoclinic
Space group	$P2_1/c$	P-1	$P2_1/n$	$P2_1/n$
a, Å	11.343(5)	10.085(5)	11.132(2)	10.9299(4)
b, Å	23.530(5)	11.118(5)	23.789(5)	23.1611(10)
c, Å	16.714(5)	18.036(5)	17.045(3)	17.1891(8)
γ, deg	90.0	98.989(5)	90.0	90.0
β, deg	109.356(5)	93.383(5)	108.57(3)	108.1320(10)
γ, deg	90.0	96.356(5)	90.0	90.0
V, Å^3	4209(2)	1979.2(14)	4279.0(15)	4135.3(3)
Z	4	2	4	4
ρ_{calcd}, g/cm^{-3}	1.556	1.345	1.449	1.609
T, K	100(2)	293(2)	293(2)	100(2)
Absorption coeff., μ,mm^{-1}	1.233	1.285	1.534	1.786
θ limits, deg	2.09 – 26.00	2.29 – 25.00	1.52 – 25.49	2.15 – 28.28
No. of measured reflections	39462	7688	31403	36308
No. of unique reflections	8264	5998	7968	10258
No. of observed reflections [$I > 2\sigma(I)$]	5852	4293	6030	7689
no. of parameters	559	440	514	550
GOF on F^2	1.017	1.043	1.041	1.048
R_1 [$I > 2\sigma(I)$]^a ,%	4.97	10.91	5.48	4.54
wR_2^b, %	12.19	26.24	17.46	11.05
max, min peaks, e/Å^3	1.255 and –0.812	3.716 and –2.168	1.919 and -0.723	2.417 and –1.531

[a] $R_1 = \Sigma||F_o|-|F_C||/ \Sigma|F_0|$; [b] $wR_2 = \{\Sigma [w(F_o^2 - F_C^2)]/ \Sigma[w(F_0^2)^2]\}^{1/2}$

Table S2. Selected bond distances (Å) and bond angles (deg) for [Pr(DTPAAQ)(DMF)]•DMF•3H_2O (**1**)

Pr(1)-O(1)	2.508(4)	O(5)-Pr(1)-O(1)	78.18(15)
Pr(1)-O(2)	2.519(4)	O(5)-Pr(1)-O(2)	77.71(15)
Pr(1)-O(3)	2.404(4)	O(2)-Pr(1)-N(3)	59.71(14)
Pr(1)-O(4)	2.422(4)	O(3)-Pr(1)-N(1)	64.89(13)
Pr(1)-O(5)	2.419(4)	O(3)-Pr(1)-N(2)	78.31(15)
Pr(1)-O(6)	2.454(4)	O(3)-Pr(1)-N(3)	138.66(14)
Pr(1)-N(1)	2.736(4)	O(5)-Pr(1)-N(1)	70.98(15)
Pr(1)-N(2)	2.698(4)	O(5)-Pr(1)-O(4)	131.32(14)
Pr(1)-N(3)	2.825(5)	O(5)-Pr(1)-O(6)	132.17(14)
O(1)-Pr(1)-O(2)	96.16(13)	O(6)-Pr(1)-O(1)	73.62(13)
O(3)-Pr(1)-O(1)	82.28(13)	O(6)-Pr(1)-O(2)	68.01(14)
O(3)-Pr(1)-O(2)	144.01(13)	O(1)-Pr(1)-N(1)	62.50(13)
O(3)-Pr(1)-O(4)	76.18(13)	O(1)-Pr(1)-N(2)	129.54(13)
O(3)-Pr(1)-O(5)	135.86(13)	O(1)-Pr(1)-N(3)	137.08(15)
O(3)-Pr(1)-O(6)	77.21(13)	O(2)-Pr(1)-N(1)	144.86(15)
O(4)-Pr(1)-O(1)	150.43(14)	O(5)-Pr(1)-N(2)	84.35(14)
O(4)-Pr(1)-O(2)	89.75(14)	O(5)-Pr(1)-N(3)	63.00(15)
O(4)-Pr(1)-O(6)	81.95(13)		

Table S3. Selected bond distances (Å) and bond angles (deg) for [Pr(DTPAAQ)(H_2O)] (**1a**)

Pr(1)-O(1)	2.464(9)	O(4)-Pr(1)-O(2)	88.2(6)
Pr(1)-O(2)	2.397(18)	O(4)-Pr(1)-O(5)	131.2(5)
Pr(1)-O(2A)	1.85(4)	O(4)-Pr(1)-O(6)	83.0(5)
Pr(1)-O(3)	1.810(16)	O(5)-Pr(1)-O(1)	77.2(4)
Pr(1)-O(3A)	2.32(4)	O(5)-Pr(1)-O(6)	133.7(4)
Pr(1)-O(4)	2.372(19)	O(3)-Pr(1)-N(1)	47.1(6)
Pr(1)-O(5)	2.409(12)	O(1)-Pr(1)-N(1)	61.8(4)
Pr(1)-O(6)	2.520(10)	O(1)-Pr(1)-N(2)	128.1(4)
Pr(1)-N(1)	2.760(12)	O(1)-Pr(1)-N(3)	134.4(3)
Pr(1)-N(2)	2.683(9)	O(2)-Pr(1)-N(1)	146.1(5)
Pr(1)-N(3)	2.798(11)	O(2)-Pr(1)-N(2)	126.7(5)
O(1)-Pr(1)-O(6)	72.4(4)	O(2)-Pr(1)-N(3)	59.1(4)
O(2)-Pr(1)-O(1)	96.3(5)	O(2A)-Pr(1)-N(1)	135.9(12)
O(2)-Pr(1)-O(5)	80.4(5)	O(2A)-Pr(1)-N(2)	120.5(12)
O(2)-Pr(1)-O(6)	69.4(5)	O(2A)-Pr(1)-N(3)	52.4(11)
O(2A)-Pr(1)-O(1)	95.1(12)	O(3)-Pr(1)-N(1)	47.1(6)
O(2A)-Pr(1)-O(2)	12.3(12)	O(3)-Pr(1)-N(2)	61.5(6)
O(2A)-Pr(1)-(3A)	155.1(15)	O(3)-Pr(1)-N(3)	129.3(5)
O(2A)-Pr(1)-O(4)	94.9(13)	O(3A)-Pr(1)-N(1)	65.0(9)
O(2A)-Pr(1)-O(5)	68.2(13)	O(3A)-Pr(1)-N(2)	77.5(9)
O(2A)-Pr(1)-O(6)	80.6(12)	O(3A)-Pr(1)-N(3)	139.4(9)
O(3)-Pr(1)-O(1)	85.2(5)	O(4)-Pr(1)-N(1)	123.7(5)
O(3)-Pr(1)-O(2)	164.2(6)	O(4)-Pr(1)-N(2)	67.0(5)
O(3)-Pr(1)-O(2A)	176.5(13)	O(4)-Pr(1)-N(3)	71.4(5)
O(3)-Pr(1)-O(3A)	21.5(9)	O(5)-Pr(1)-N(1)	70.1(4)
O(3)-Pr(1)-O(4)	83.3(7)	O(5)-Pr(1)-N(2)	82.6(4)
O(3)-Pr(1)-O(5)	115.2(6)	O(5)-Pr(1)-N(3)	62.1(4)
O(3)-Pr(1)-O(6)	96.3(6)	O(6)-Pr(1)-N(1)	120.9(3)
O(3A)-Pr(1)-O(1)	84.2(9)	O(6)-Pr(1)-N(2)	143.7(4)
O(3A)-Pr(1)-O(2)	142.8(10)	O(6)-Pr(1)-N(3)	122.1(3)
O(3A)-Pr(1)-O(4)	75.6(10)	N(1)-Pr(1)-N(3)	116.5(3)
O(3A)-Pr(1)-O(5)	135.0(9)	N(2)-Pr(1)-N(1)	66.4(3)
O(3A)-Pr(1)-O(6)	75.4(9)	N(2)-Pr(1)-N(3)	68.3(4)
O(4)-Pr(1)-O(1)	151.5(5)		

Table S4. Selected bond distances (Å) and bond angles (deg) for [Eu(DTPAAQ)(DMF)]•3H_2O (**2**•3H_2O)

Eu(1)-O(1)	2.453(4)	O(4)-Eu(1)-O(6)	79.66(18)
Eu(1)-O(2)	2.486(5)	O(5)-Eu(1)-O(1)	76.59(18)
Eu(1)-O(3)	2.348(5)	O(5)-Eu(1)-O(2)	77.98(19)
Eu(1)-O(4)	2.366(4)	O(5)-Eu(1)-O(3)	136.00(18)
Eu(1)-O(5)	2.339(5)	O(5)-Eu(1)-O(4)	132.53(18)
Eu(1)-O(6)	2.394(5)	O(5)-Eu(1)-O(6)	132.62(19)
Eu(1)-N(1)	2.689(6)	O(6)-Eu(1)-O(1)	73.86(17)
Eu(1)-N(2)	2.636(5)	O(6)-Eu(1)-O(2)	67.59(18)
Eu(1)-N(3)	2.759(6)	O(2)-Eu(1)-N(3)	60.38(17)
O(1)-Eu(1)-O(2)	93.00(16)	O(3)-Eu(1)-N(1)	65.32(18)
O(3)-Eu(1)-O(1)	84.53(18)	O(5)-Eu(1)-N(3)	63.99(19)
O(3)-Eu(1)-O(2)	143.16(17)	O(6)-Eu(1)-N(1)	123.86(18)
O(3)-Eu(1)-O(4)	76.40(17)	O(6)-Eu(1)-N(2)	140.73(19)
O(3)-Eu(1)-O(6)	76.50(18)	O(6)-Eu(1)-N(3)	118.78(18)
O(4)-Eu(1)-O(1)	150.33(17)	N(1)-Eu(1)-N(3)	117.13(18)
O(4)-Eu(1)-O(2)	89.04(17)		

Table S5. Selected bond distances (Å) and bond angles (deg) for [Tb(DTPAAQ)(DMF)]•DMF•3H_2O (**3**•DMF•3H_2O).

Tb(1)-O(1)	2.419(3)	O(6)-Tb(1)-O(1)	72.92(11)
Tb(1)-O(2)	2.463(3)	O(6)-Tb(1)-O(2)	67.39(11)
Tb(1)-O(3)	2.334(3)	O(1)-Tb(1)-N(1)	64.06(11)
Tb(1)-O(4)	2.338(3)	O(1)-Tb(1)-N(2)	132.20(11)
Tb(1)-O(5)	2.327(3)	O(1)-Tb(1)-N(3)	137.44(12)
Tb(1)-O(6)	2.358(3)	O(2)-Tb(1)-N(1)	143.15(11)
Tb(1)-N(1)	2.662(4)	O(2)-Tb(1)-N(3)	61.48(11)
Tb(1)-N(2)	2.626(4)	O(3)-Tb(1)-N(1)	66.08(11)
Tb(1)-N(3)	2.728(4)	O(3)-Tb(1)-N(2)	75.74(12)
O(1)-Tb(1)-O(2)	91.42(10)	O(3)-Tb(1)-N(3)	137.02(12)
O(3)-Tb(1)-O(1)	84.70(11)	O(4)-Tb(1)-N(1)	126.25(11)
O(3)-Tb(1)-O(2)	142.53(11)	O(4)-Tb(1)-N(2)	67.47(12)
O(3)-Tb(1)-O(4)	74.91(11)	O(4)-Tb(1)-N(3)	69.95(12)
O(3)-Tb(1)-O(6)	75.90(11)	O(5)-Tb(1)-N(1)	71.56(12)
O(4)-Tb(1)-O(1)	147.08(11)	O(5)-Tb(1)-N(2)	88.27(13)
O(4)-Tb(1)-O(2)	89.51(11)	O(5)-Tb(1)-N(3)	65.17(13)
O(4)-Tb(1)-O(6)	77.15(11)	O(6)-Tb(1)-N(1)	123.79(11)
O(5)-Tb(1)-O(1)	77.55(12)	O(6)-Tb(1)-N(3)	117.98(12)
O(5)-Tb(1)-O(2)	76.70(12)	N(1)-Tb(1)-N(3)	118.12(12)
O(5)-Tb(1)-O(3)	137.64(12)	N(2)-Tb(1)-N(1)	68.14(12)
O(5)-Tb(1)-O(4)	134.33(12)	N(2)-Tb(1)-N(3)	68.50(12)
O(5)-Tb(1)-O(6)	132.12(12)		

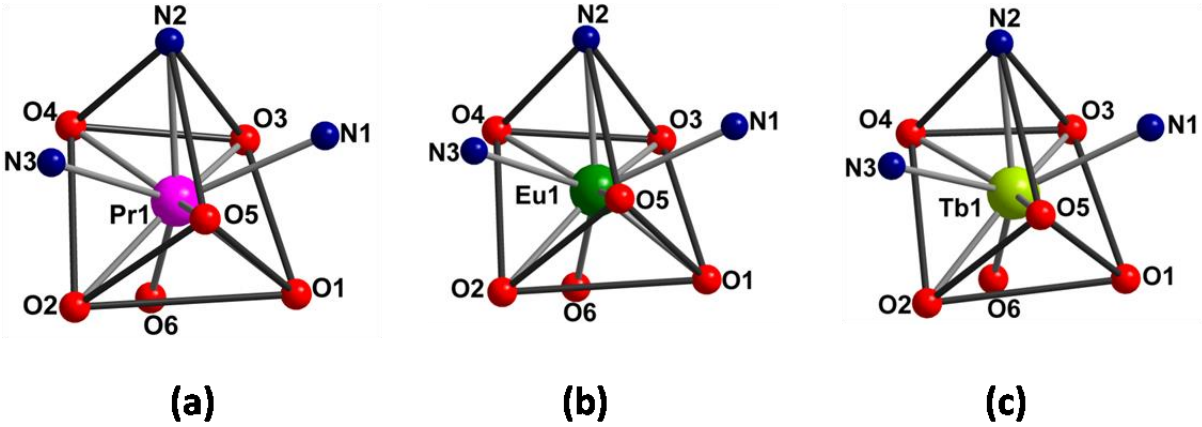

Figure S9. Coordination polyhedra of the nine-coordinate {LnN_3O_6} lanthanide cores showing tricapped-trigonal prism (TTP) coordination geometry in complexes **1** (a), **2** (b), and **3** (c).

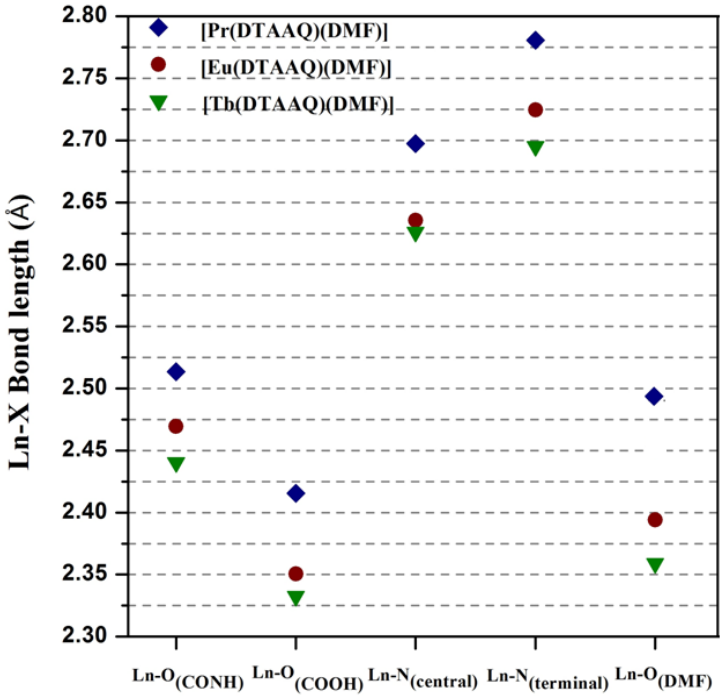

Figure S10. Variation of Ln-X (X=O, N) bond lengths in [Ln(DTPAAQ)(DMF)] (**1-3**) for $\{LnN_3O_6\}$ core. Average bond distances were taken from similar set of bonds.

Respective bond distances are shown in table below.

Bond Distance	**[Pr(DTPAAQ)(DMF)] (1)**	**[Eu(DTPAAQ)(DMF)] (2)**	**[Tb(DTPAAQ)(DMF)] (3)**
Ln-O1 (CONH)	2.508(4)	2.453(4)	2.419(3)
Ln-O2 (CONH)	2.519(4)	2.486 (5)	2.463(3)
Ln-O3 (COOH)	2.404(4)	2.348(5)	2.334(3)
Ln-O4 (COOH)	2.422(4)	2.366(4)	2.338(3)
Ln-O5 (COOH)	2.421(4)	2.339(5)	2.327(3)
Ln-N(NCH_2CH_2**N2**CH_2CH_2N)	2.697(4)	2.636(5)	2.625(4)
Ln -N(-$NHCH_2CH_2$**N1**CH_2CH_2N-)	2.737(4)	2.689(6)	2.662(4)
Ln -N(-$NHCH_2CH_2$**N3**CH_2CH_2N-)	2.824(5)	2.759(6)	2.728(4)
Ln-O(DMF)	2.453(4)	2.394(5)	2.358(3)

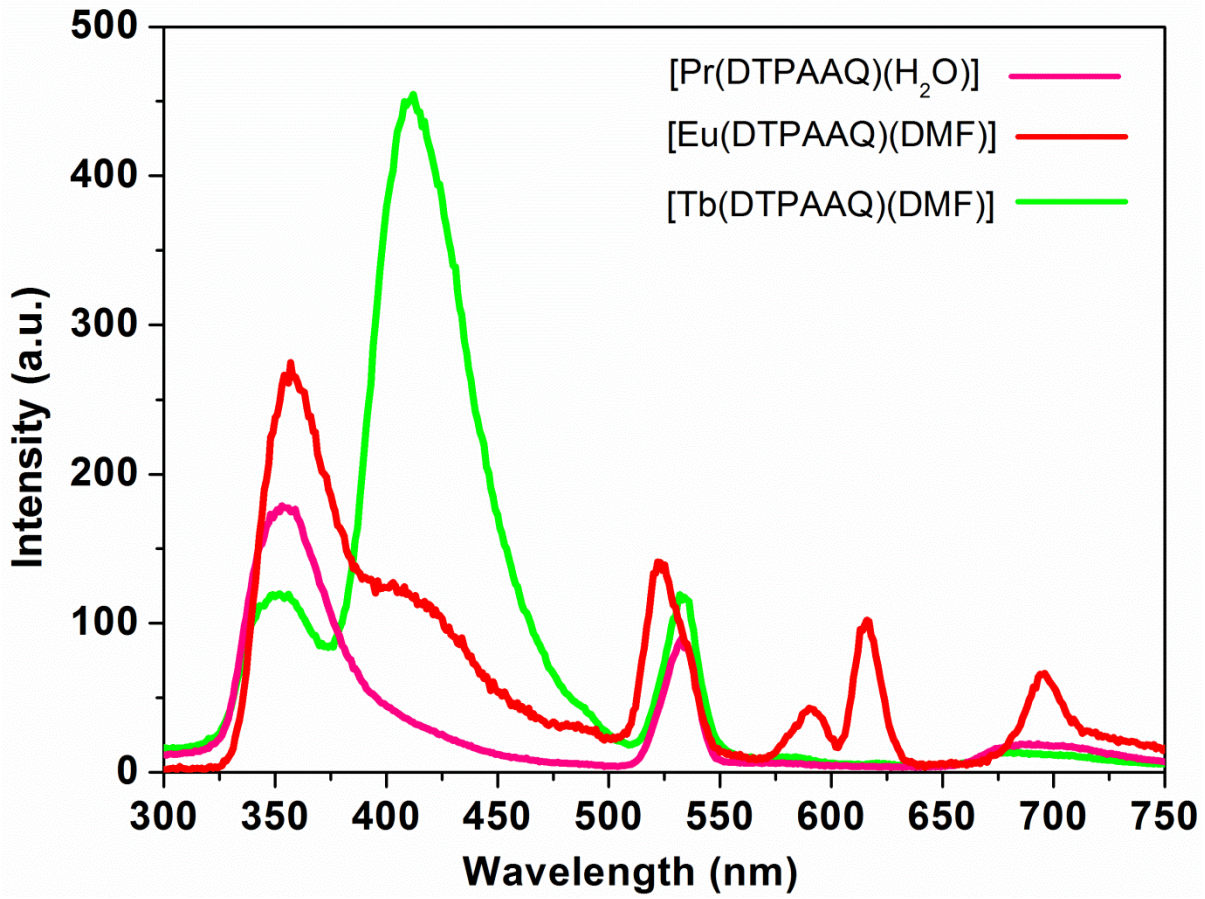

Figure S11. Overlay of steady state luminescence spectra of **[**Pr(DTPAAQ)(DMF)] (**1**), [Eu(DTPAAQ)(DMF)] (**2**), and [Tb(DTPAAQ)(DMF)] (**3**) in aqueous - DMF at λ_{ex}= 262 nm with slit width of 5 nm. *Note: The band at 524 nm arises due to second order Rayleigh scattering.*

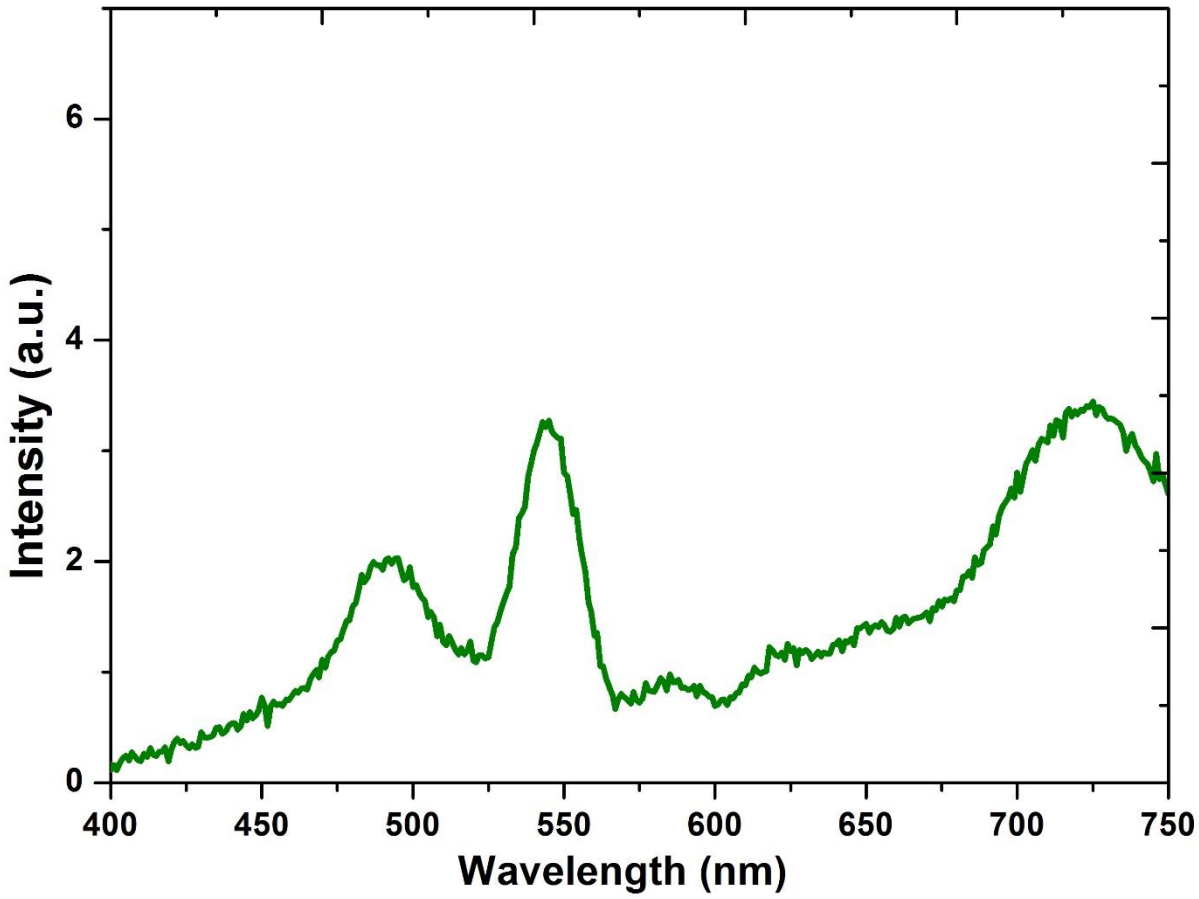

Figure S12. Time-resolved luminescence spectra of **[**Pr(DTPAAQ)(DMF)] (**1**) in in DMF at 298 K. Delay time = 0.1 ms, λ_{ex} = 330 nm, slit width= 5 nm.

Table S6. Luminescence lifetime (τ)[a] , determination of inner-sphere hydration number (q) [b] of the complexes in H_2O and D_2O.

Complex	λ_{ex} (nm)	τ^{H_2O} (ms)	τ^{D_2O} (ms)	q
[Eu(DTPAAQ)(DMF)] (**2**)	330 nm	0.64	1.81	0.92
[Tb(DTPAAQ)(DMF)] (**3**)	330 nm	0.51	0.58	0.88

[a] luminescence lifetime measured from decay curve profile from $^5D_0$ and $^5D_4$ excited states at 616 nm and 545 nm for Eu^{3+} and Tb^{3+} complexes respectively within experimental uncertainty of ± 10%. [b]q is the number of water molecules coordinated to Ln^{3+} ion in solution measured from modified Horrock's equation[42] described in experimental section of manuscript.

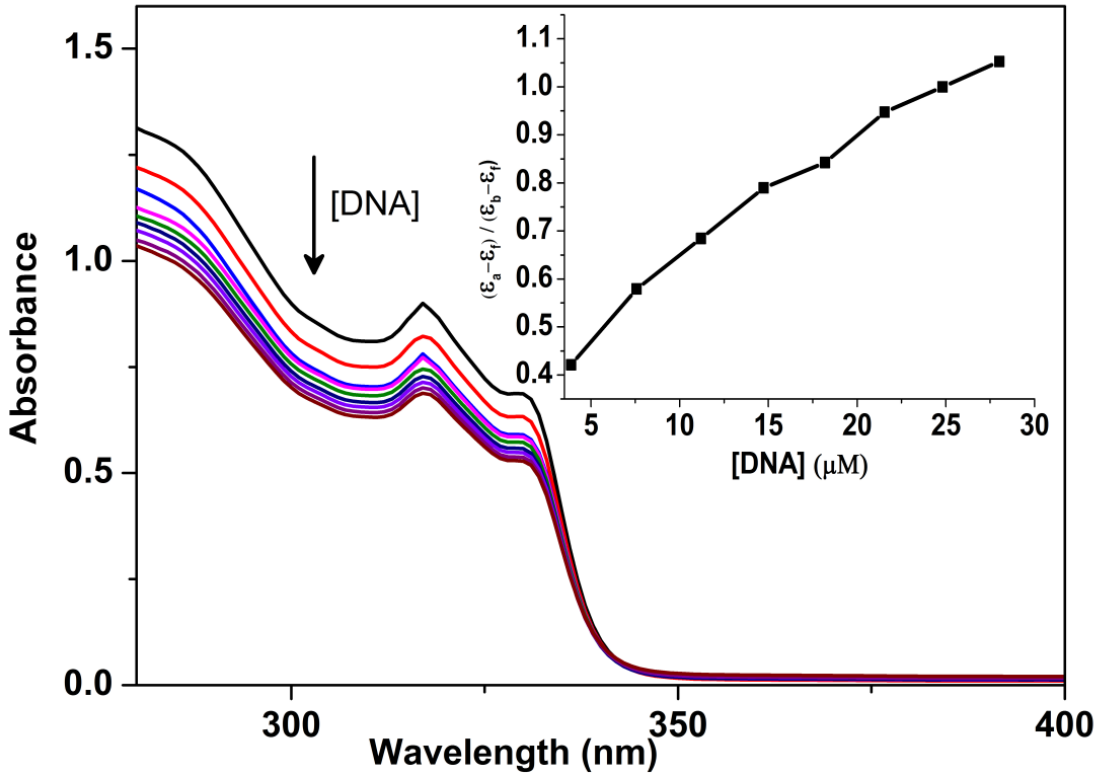

Figure S14. Absorption spectral traces of complex **1** in 5 mM Tris-HCl buffer (pH 7.2) on increasing amount of CT-DNA to solution of **1**. Inset figure shows plot of [DNA] versus {($\varepsilon_a - \varepsilon_f$)/($\varepsilon_b - \varepsilon_f$)}.

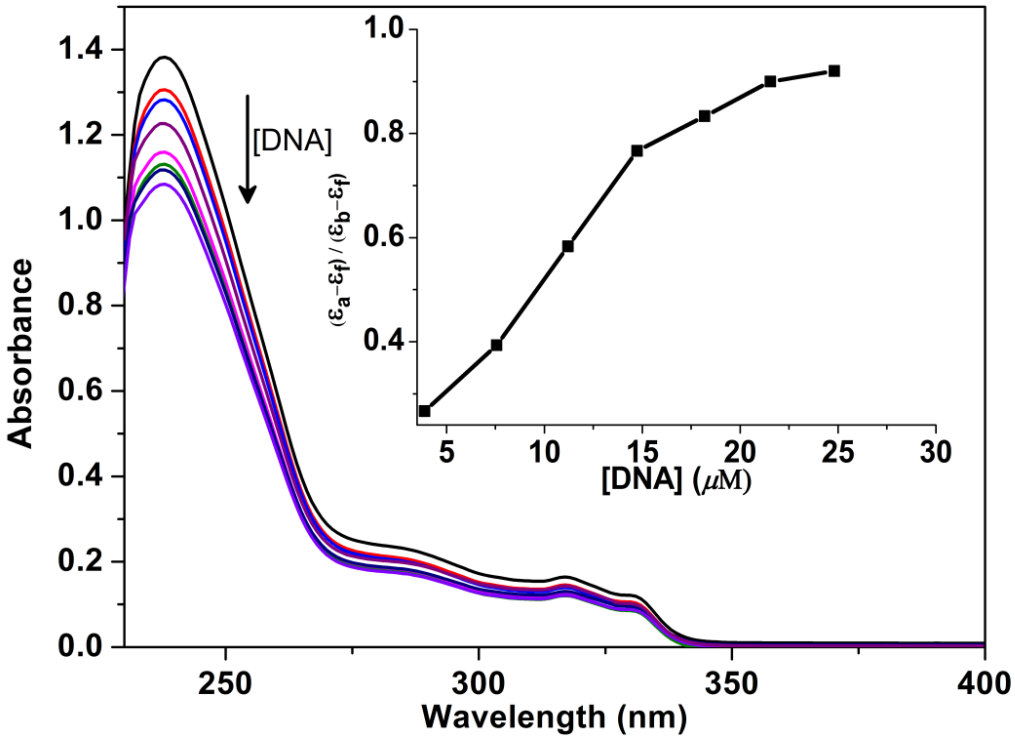

Figure S15. Absorption spectral traces of complex **2** in 5 mM Tris-HCl buffer (pH 7.2) on increasing amount of CT-DNA to a solution of **2**. Inset figure shows plot of [DNA] versus {($\varepsilon_a - \varepsilon_f$)/($\varepsilon_b - \varepsilon_f$)}.

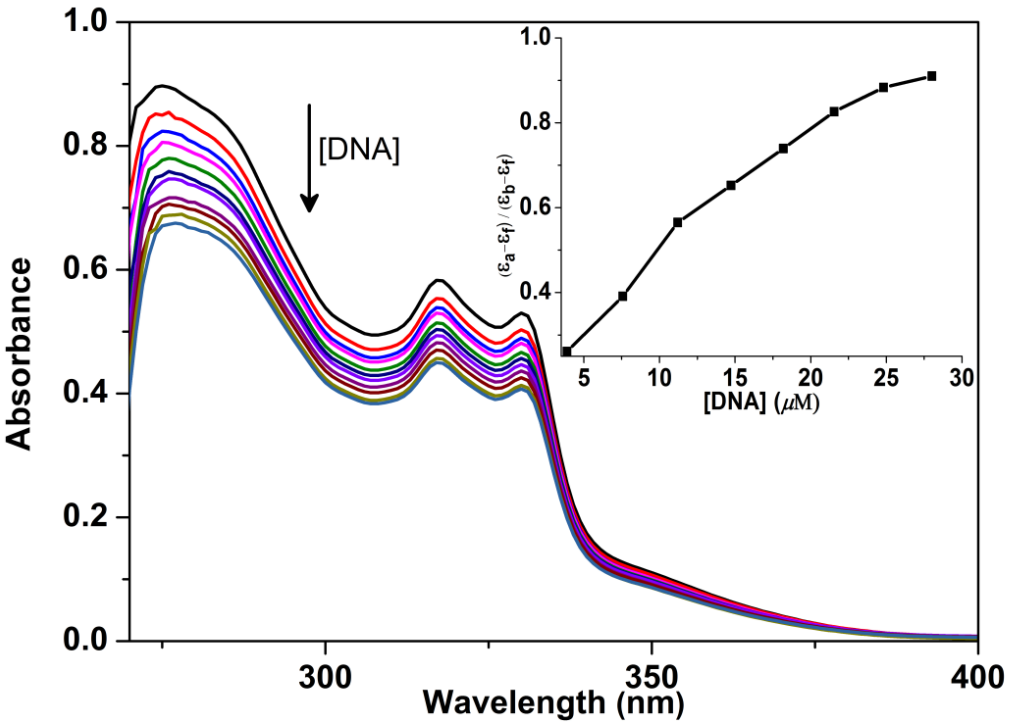

Figure S16. Absorption spectral traces of complex **3** in 5 mM Tris-HCl buffer (pH 7.2) on increasing amount of CT-DNA to solution of **3**. Inset figure shows plot of [DNA] versus $\{(\varepsilon_a - \varepsilon_f)/(\varepsilon_b - \varepsilon_f)\}$.

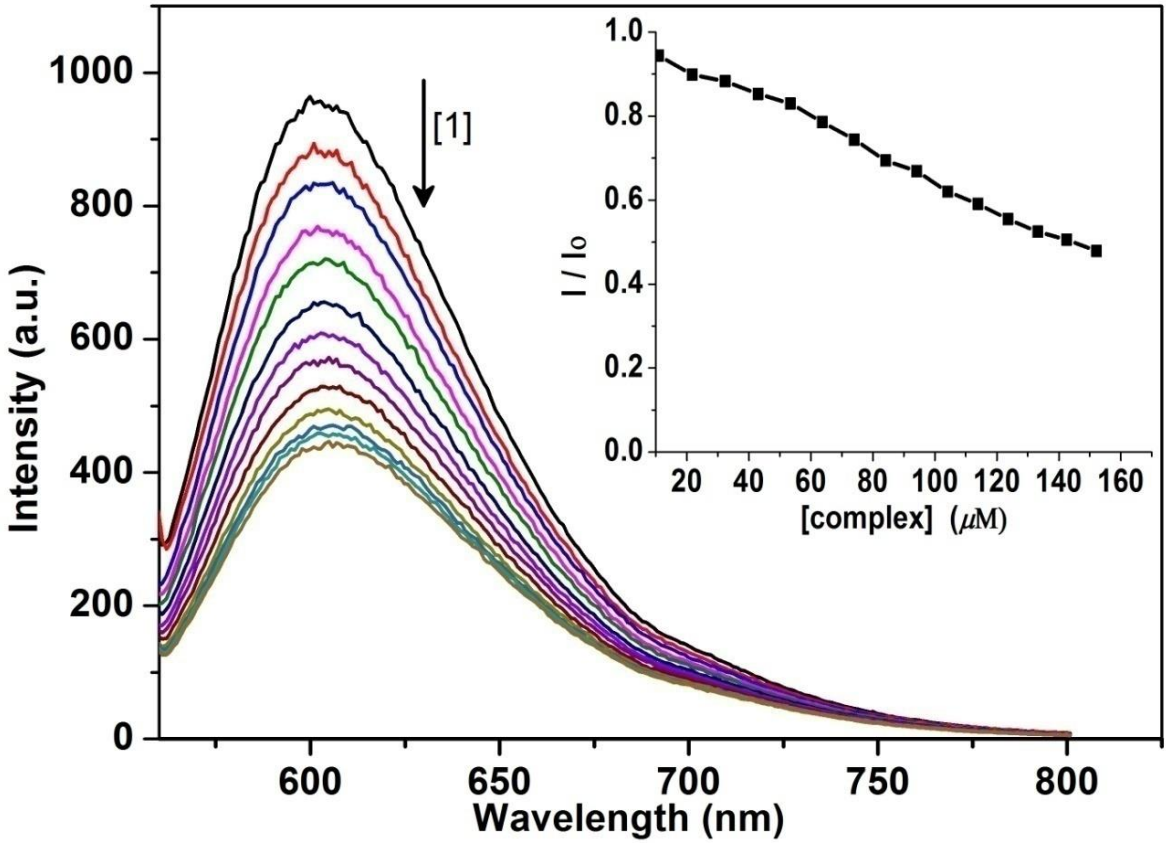

Figure S17. Emission spectral overlay plot for CT- bounded ethidium bromide (3 μM) in Tris -HCl buffer (5 mM, pH 7.2) with increasing concentration of [Pr(DTPAAQ)(DMF)] (**1**).

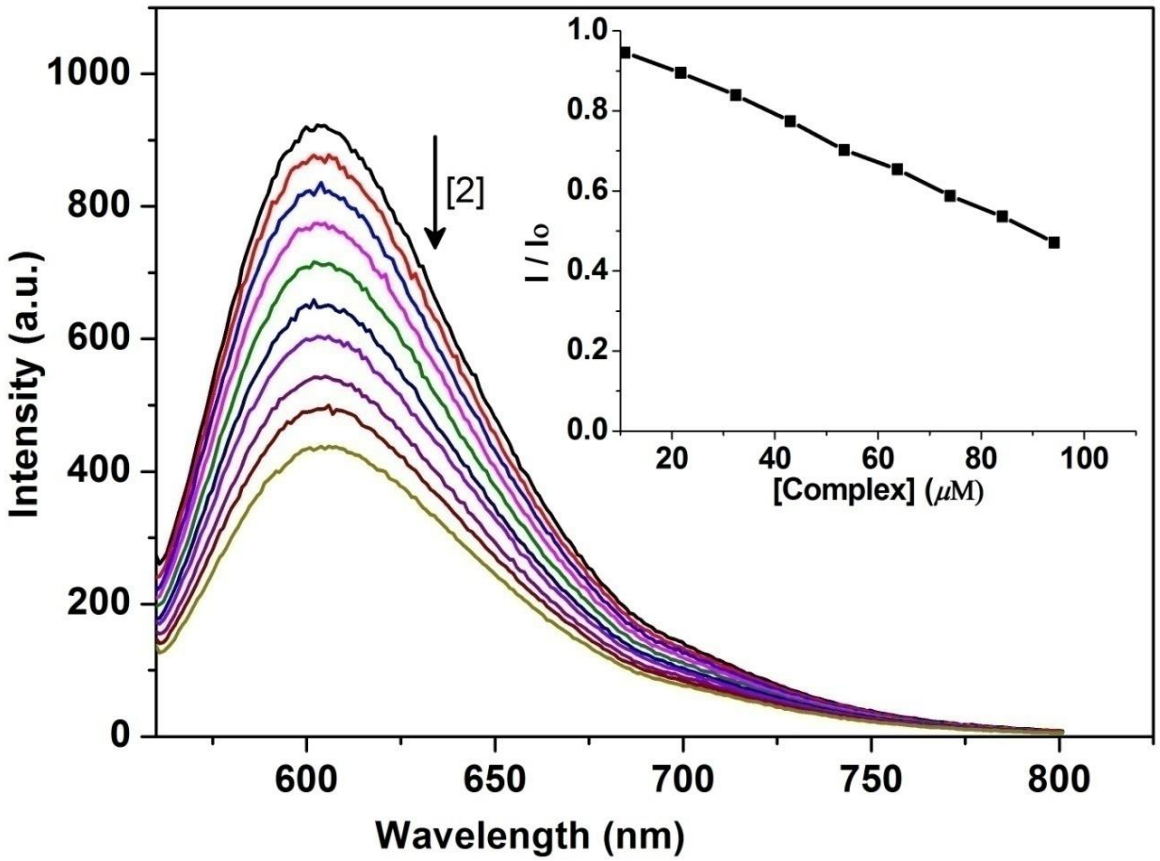

Figure S18. Emission spectral overlay plot for CT-bounded ethidium bromide (3 μM) in Tris-HCl buffer (5mM, pH7.2) with increasing concentration of [Pr(DTPAAQ)(DMF)] (**2**).

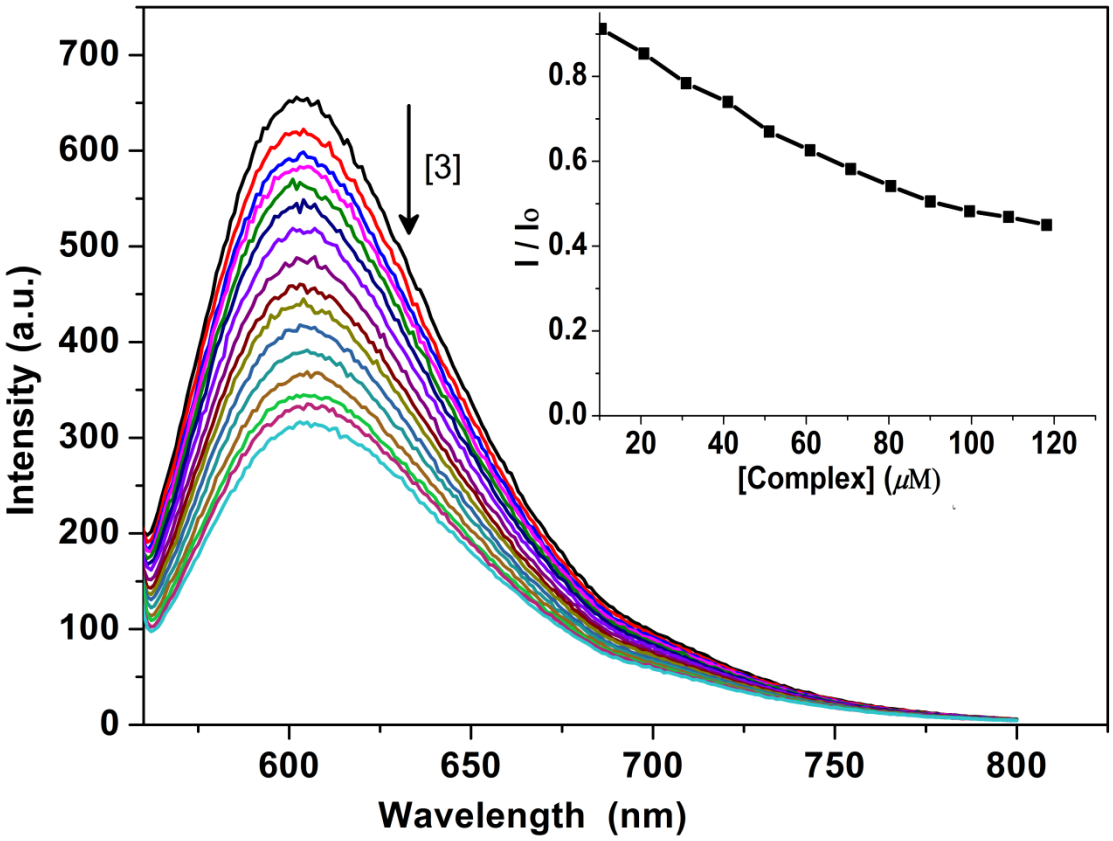

Figure S19. Emission spectral overlay plot for CT-DNA bounded ethidium bromide (3 μM) in Tris HCl-NaCl buffer (5mM, pH7.2) with increasing concentration of [Tb(DTPAAQ)(DMF)] (**3**).

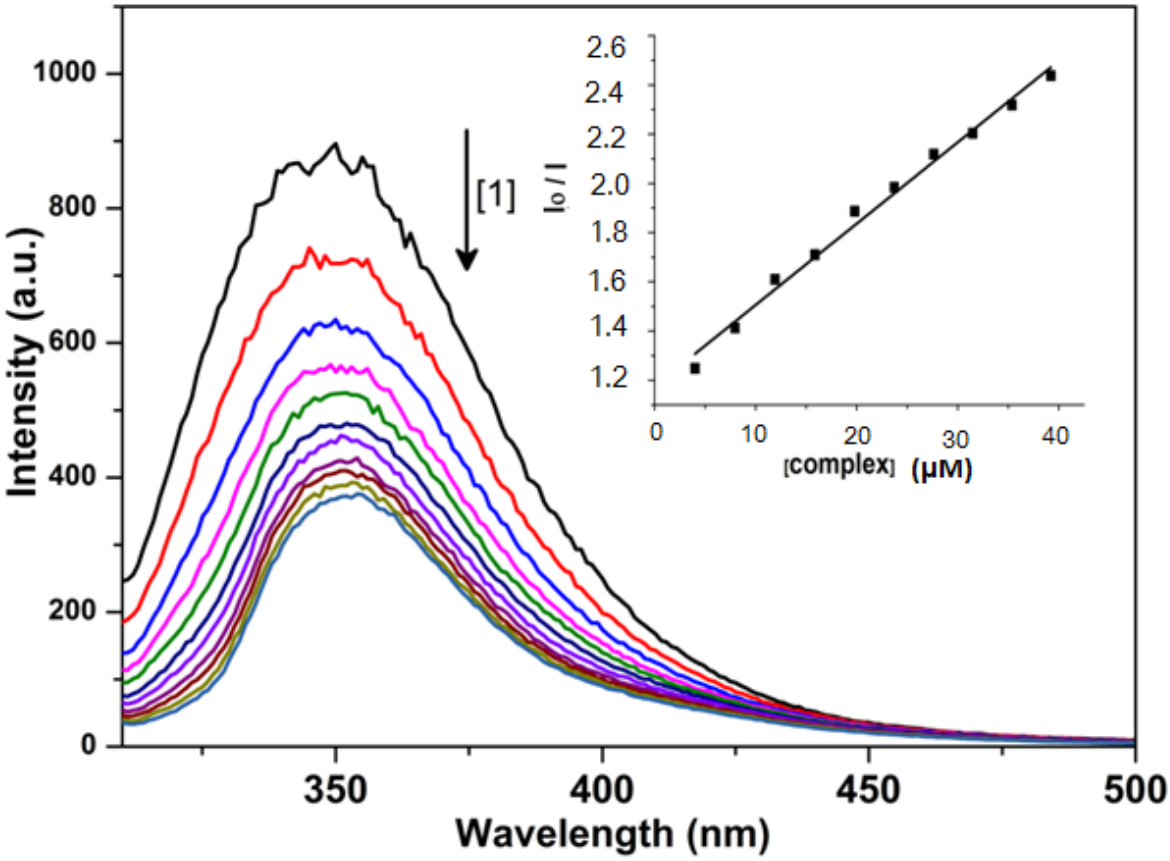

Figure S20. The effect of increasing concentration of [Pr(DTPAAQ)(DMF)] (**1**) on the fluorescence quenching of BSA (2 μM) in Tris HCl- NaCl (5mM, pH 7.2). λ_{ex} = 295 nm, λ_{em} = 340 nm. The Inset shows the plot of I_0/I *vs.* [complex].

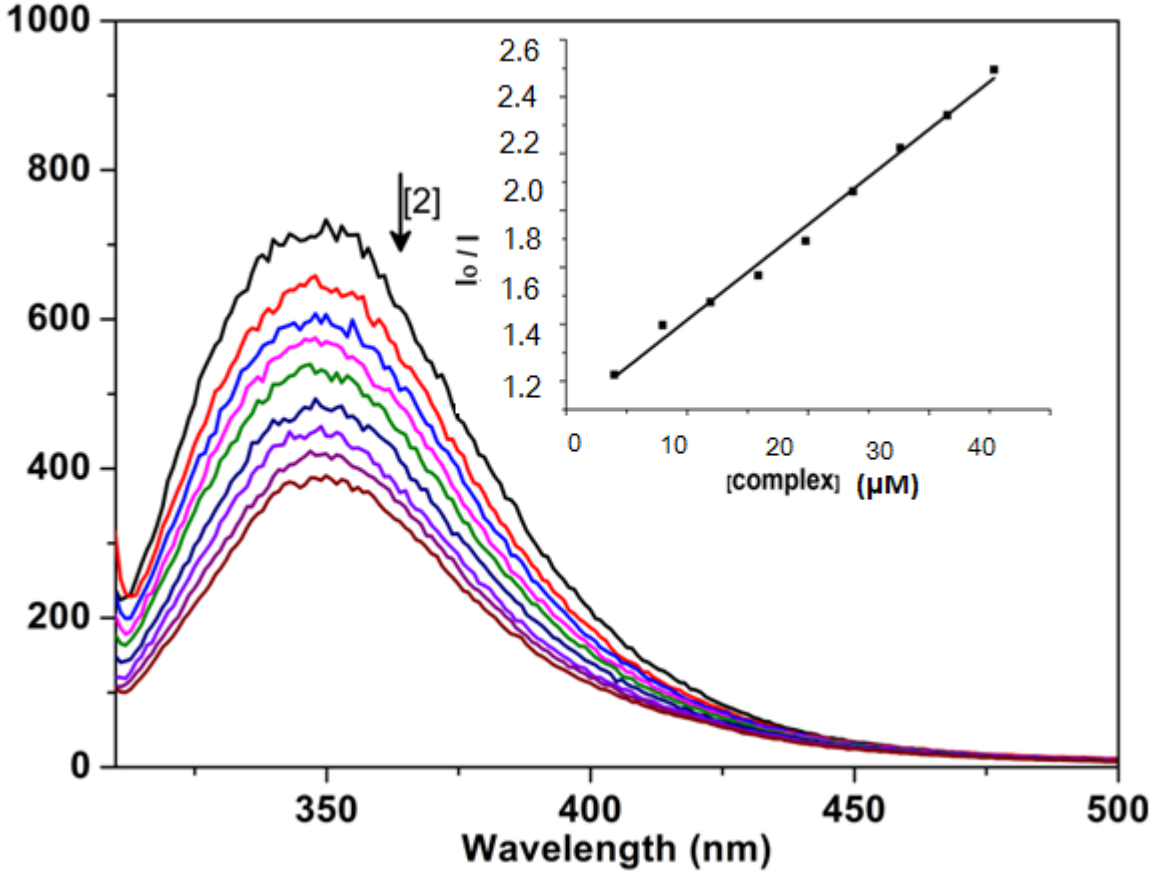

Figure S21. The effect of increasing concentration of [Eu(DTPAAQ)(DMF)] (**2**) on the fluorescence quenching of BSA (2 μM) in Tris HCl- NaCl (5mM, pH 7.2). λ_{ex} = 295 nm, λ_{em} = 340 nm. The Inset shows the plot of I_0/I *vs.* [complex].

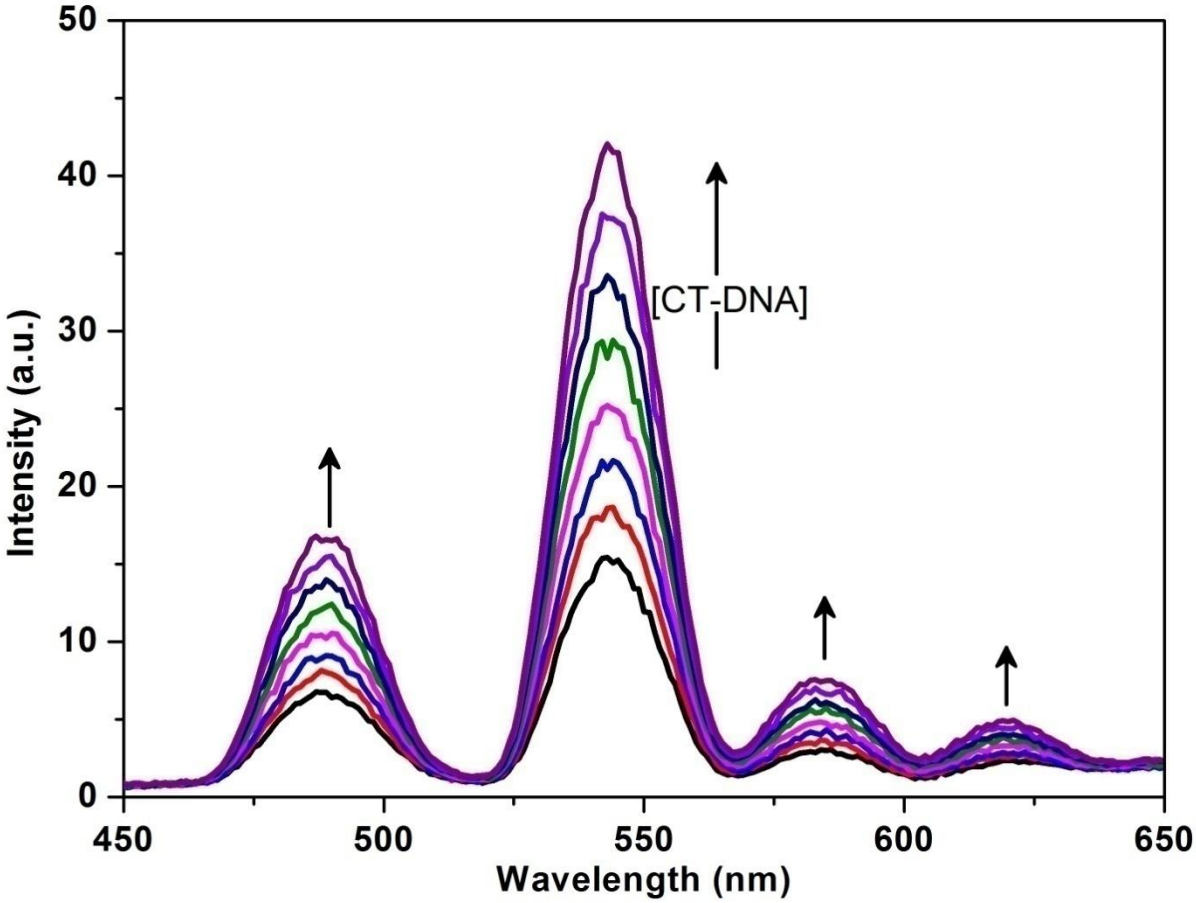

Figure S22. Time resolved luminescence spectra of complex [Tb(DTPAAQ)(DMF)] (**3**) (delay time = 0.1 ms, λ_{ex} = 330 nm) in response to increasing concentration of CT-DNA in Tris HCl-NaCl buffer (5 mM, pH 7.2) at 298 K.

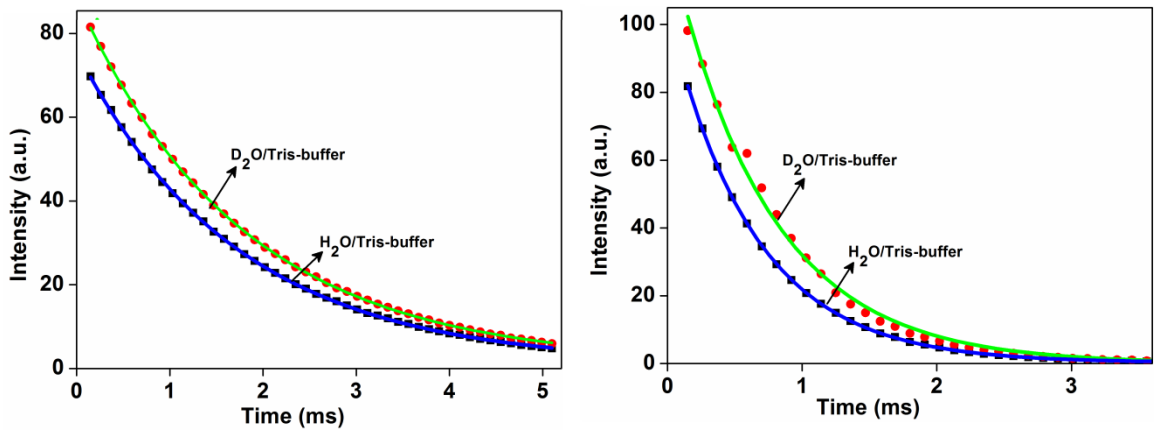

Figure S23. Luminescence decay profile from $^5D_0$ state of Eu(III) in complex **2** and from $^5D_4$ of Tb in complex **3** at λ_{em} = 616 nm and 543 nm (λ_{ex} = 330 nm) respectively in presence of CT-DNA in 5 mM Tris buffer in water (blue) and in D_2O (green). [**2**] = 40 μM, [DNA] = 60 μM, delay time and gate time = 0.1 ms, Ex. and Em. slit = 10 nm. The solid lines are the best fits considering single-exponential behaviour of the decay.

Table S7. Luminescence lifetime (τ)[a] , determination of inner-sphere hydration number (q) in presence of CT-DNA.[a]

Complex	λ_{ex} (nm)	τ Tris buffer in H_2O (ms)[b]	τ Tris buffer in D_2O (ms)[c]	q
[Eu(DTPAAQ)(DMF)] (**2**)	330 nm	0.950	1.760	0.290
[Tb(DTPAAQ)(DMF)] (**3**)	330 nm	0.565	0.596	0.160

[a] [complex] = 40 µM, [DNA] = 60 µM, [b] In 5 mM Tris-HCl/NaCl buffer in Milli-Q water (pH 7.2). [c] In 5 mM Tris-HCl/NaCl buffer in D_2O.

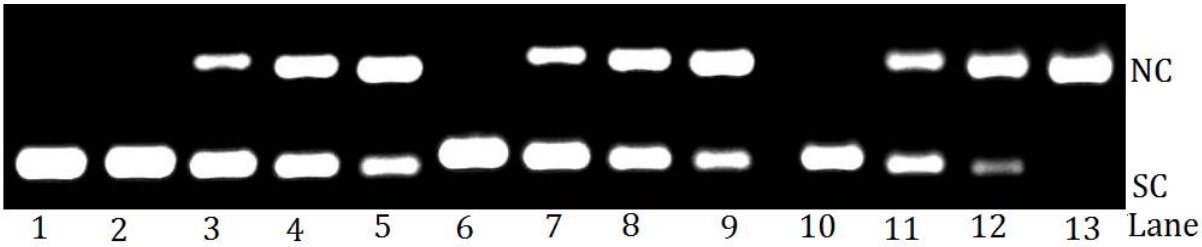

Figure S24. Cleavage of SC pUC19 DNA (0.2 μg) by the complexes **1-3** at 100 μM concentration in Tris-HCl/NaCl buffer (pH, 7.2) on photo-irradiation in UV-light at 312 nm for varying time of photoexposure.

SI. No.	Reaction condition	*t* / min	SC(%)	NC(%)
1.	DNA control	60	96	4
2.	DNA + complex **1**	0	97	3
3	DNA + complex **1**	20	75	25
4	DNA + complex **1**	40	50	50
5	DNA + complex **1**	60	29	71
6	DNA + complex **2**	0	96	4
7	DNA + complex **2**	20	70	30
8	DNA + complex **2**	40	51	59
9	DNA + complex **2**	60	27	73
10	DNA + complex **3**	0	95	5
11	DNA + complex **3**	20	53	47
12	DNA + complex **3**	40	23	77
13	DNA + complex **3**	60	5	95